

# Pyrolysis-derived waste polypropylene oils in gas turbine engines: a comprehensive performance and emission study

TOMASZ KACPER SUCHOCKI<sup>a,\*</sup>  
PAWEŁ KAZIMIERSKI<sup>a</sup>  
KATARZYNA JANUSZEWICZ<sup>b</sup>  
PIOTR LAMPART<sup>a</sup>  
DAWID ZANIEWSKI<sup>a</sup>  
PIOTR KLIMASZEWSKI<sup>a</sup>  
ŁUKASZ WITANOWSKI<sup>a</sup>

<sup>a</sup> Institute of Fluid Flow Machinery, Polish Academy of Sciences,  
Fiszera 14, 80-231 Gdańsk, Poland

<sup>b</sup> Gdańsk University of Technology, Narutowicza 11/12, 80-233 Gdańsk,  
Poland

**Abstract** Addressing the burgeoning issue of polymer waste management and disposal, chemical recycling, specifically the production of high-quality oil, presents an enticing solution. This research paper delves into the process of plastic waste pyrolysis, focusing on polypropylene, and thoroughly examines the physico-chemical properties of the resulting pyrolytic oil. The oils, obtained from waste plastic pyrolysis (referred to as WPPO), are then blended with kerosene and utilized as fuel for a gas turbine engine. The primary objective of this investigation is to ascertain how the blend composition influences the performance and emission parameters of the micro gas turbine. In our findings, it was observed that all tested waste plastic pyrolysis blends displayed a trend towards escalating regulated emissions such as nitrogen oxides (NO<sub>x</sub>) with an average increase of 26% for polypropylene pyrolysis oil (PPO). The emission index (EI) for carbon monoxide (CO) was found to be relatively consistent across all fuel blends tested in this study. Interestingly, when considering the thrust specific fuel consumption (TSFC) within the EI calculation, blends of aviation kerosene and plastic oil showed

---

\*Corresponding Author. Email: [tsuchocki@imp.gda.pl](mailto:tsuchocki@imp.gda.pl)

lower values in comparison to the pure Jet A-1 fuel. Furthermore, an augmentation in the proportion of WPPO in the blends consequently led to an elevation in the exhaust gas temperature (an average increase of 8.7% for PPO). Interestingly, the fuel efficiency of the Jet engine, expressed as TSFC, demonstrated a decrease, with an average reduction of 13.8% observed for PPO.

**Keywords:** Waste plastic pyrolysis oil; Gas turbine engine; Polypropylene; Emissions; Performance

### Nomenclature

|               |   |  |
|---------------|---|--|
| EGT           | – | exhaust gas temperature, °C                        |
| $El_i$        | – | gas species ( $i$ ) emission index                 |
| $El_{i,\tau}$ | – | gas species ( $i$ ) thrust specific emission index |
| HHV           | – | higher heating value, MJ/kg                        |
| LHV           | – | lower heating value, MJ/kg                         |
| $\dot{m}_f$   | – | fuel mass flow rate, kg/s                          |
| $\dot{m}_i$   | – | gas species ( $i$ ) mass flow rate, kg/s           |
| $MW_f$        | – | fuel molecular weight, kg/mol                      |
| $MW_i$        | – | gas species ( $i$ ) molecular weight, kg/mol       |
| TSFC          | – | thrust specific fuel consumption, kg/sN            |
| $x$           | – | number of carbon atoms in the fuel molecule        |

### Greek symbols

|               |   |                                   |
|---------------|---|-----------------------------------|
| $\chi_{CO}$   | – | carbon monoxide mole fraction     |
| $\chi_{CO_2}$ | – | carbon dioxide mole fraction      |
| $\chi_i$      | – | gas species ( $i$ ) mole fraction |
| $\tau$        | – | static thrust, N                  |

### Abbreviations

|                              |   |   |
|------------------------------|---|---|
| CHP                          | – | combined heat and power   |
| CO                           | – | carbon monoxide   |
| CO <sub>2</sub>              | – | carbon dioxide  |
| NO <sub><math>x</math></sub> | – | nitrogen oxides   |
| HDPE                         | – | high-density polyethylene   |
| HEFA                         | – | hydro-processed esters and fatty acids                                |
| LPDE                         | – | low-density polyethylene  |
| PE                           | – | polyethylene  |
| PET                          | – | polyethylene terephthalate  |
| PP                           | – | polypropylene   |
| PS                           | – | polystyrene   |
| PPO                          | – | polypropylene pyrolysis oil   |
| PP25, PP50, PP75, PP100      | – | blend of PPO with Jet A with 25%, 50%, 75%, 100% of PPO, respectively |
| PVC                          | – | polyvinyl chloride  |
| TPO                          | – | tyre pyrolysis oil  |
| UHC                          | – | unburned hydrocarbons   |
| WPPO                         | – | waste plastic pyrolysis oil   |

## 1 Introduction

Alternative fuels derived from plastic waste have emerged as a potent solution for waste management, while concurrently serving as a viable substitute for fossil fuels. This burgeoning market of alternative fuels bolsters energy independence, given the local availability, ease of storage, predictable quantities, and versatility of waste in meeting a diverse array of energy needs through various energy conversion technologies [1, 2]. The transition from fossil fuels to biofuels or fuels generated from plastic waste is particularly pertinent for small-scale cogeneration heat and power (CHP) plants [3, 4].

A prevailing trend in waste management is the utilization of waste polymers as alternative fuels [5, 6]. Polymers, notably plastics, constitute a significant group of materials employed across various sectors, including electronics, logistics, automotive, and healthcare. In 2019, global plastic production was approximately 368 million tons, with Europe contributing 57.9 million tons [7]. It is estimated that 38% of this was landfilled, 26% recycled, and 36% processed for energy production [8]. The substantial proportion of waste not recycled presents an economically unfavourable scenario due to its prolonged natural decomposition and a high potential for reuse.

Discarded plastics, rich in hydrocarbons, serve as excellent sources of alternative fuels due to their abundant availability and the environmental implications of their disposal [9]. The conversion of plastic waste into fuel, a promising solution, can be achieved through thermal degradation processes such as pyrolysis, gasification, combustion, hydrocracking, or catalytic cracking [10, 11]. Pyrolysis, a thermal degradation process that occurs in an oxygen-free environment, yields oil, gas, and a solid residue – char [12]. The quality of the products derived from the pyrolysis process is contingent on the raw materials, the pyrolysis reactor, and process parameters (temperature, residence time, and catalyst) [13, 14]. The liquid fraction – pyrolytic oil can be utilized in various applications such as furnaces, boilers, turbines, and diesel engines without necessitating upgrading or treatment.

The use of the rapid heating process has a positive effect on the increase in volatile fraction. The long residence time during the process allows for the degradation of long chains, which results in an increase in the content of short-chain hydrocarbons [15]. The process temperature above 800°C affects the degradation of polymer hydrocarbon chains, secondary conversion as well as obtaining an increased amount of carbon (approx. 30%) and gas composed of light hydrocarbons such as methane, ethane and propane [15].

The temperature of about 400–500°C allows us to obtain the oil fraction rich in long-chain hydrocarbons, over 80% [16]. The aim of this work is to obtain a large amount of oil, to use as a potential fuel. The performed works are an attempt to perform experiments on a quarter technical scale.

Various studies have been conducted during recent years on pyrolysis oils used as fuels, specifically for diesel engines. Waste plastic pyrolysis oils (WPPO) offered good performance and high efficiency in compression-ignition engines across a wide range of engine loads. Several useful data available in the literature on the performance of diesel engines supplied by blends of waste plastic pyrolysis oil and diesel, with the emissions of harmful exhaust components are gathered in Table 1. The presented results report a generally increasing tendency in CO, NO<sub>x</sub>, and unburned hydrocarbons (UHC) emissions with a growing content of plastic oil in diesel fuel [12, 17–20]. However, in some cases, emissions of CO and NO<sub>x</sub> were also found to decrease [21].

The use of pyrolysis oils in various power generation units, including gas turbines was conceptualized in [24]. Compact dimensions and reduced weight of turbine engines compared to diesel engines encourage was use in stationary power plants. The advantages of gas turbines over piston combustion engines are: fewer moving parts, the absence of friction components, lower maintenance costs, lower vibration and noise levels, low consumption of lubricating oil as well as low maintenance costs [25]. In spite of encouraging research results on the use of pyrolysis oils from used plastics in diesel engines, there are only a few papers published in recent years reporting experimental tests with gas turbines supplied by waste- and biomass-based fuels. Suchocki *et al.* [26] described the process of pyrolysis of waste tyres and the application of the obtained liquid fraction – tyre pyrolysis oil (TPO) for the supply of gas turbines in mixtures with aviation fuel – kerosene (Jet A). TPO was found to have parameters like density, viscosity and higher heating value (HHV) similar to those of Jet A. The authors observed that all tested blends of TPO/Jet A involved somewhat more blended fuel than pure Jet A so as to obtain similar values of static thrust, resulting in a slightly increased thrust specific fuel consumption (TSFC). The emissions of NO<sub>x</sub> and CO were found higher for all tested TPO/Jet A blends in comparison to those of Jet A.

Fast pyrolysis bio-oil (FPBO) was studied as fuel in a small scale non-regenerated micro gas turbine by Buffi *et al.* [27]. The presence of pyrolysis oil in fuel blends has a significant influence on CO and NO<sub>x</sub> emissions, as compared to pure ethanol or diesel oil. The gas turbine had a higher overall

Table 1: Literature survey on the performance and emissions of diesel engines supplied by blends of WPPO and diesel.

| Reference                             | Fuel  | Engine type  | Impact on  |  |
|---------------------------------------|---|--|--|--|
|                                       |   |  | Combustion/Performance   | Emissions  |
| Januszewicz <i>et al.</i> [22] (2023) | Polypropylene oil (PPO) and polystyrene oil (PSO)   | AVL 5402 four-stroke, single-cylinder, DI Diesel engine                        | Higher WPPO fraction led to: heat release rate $\uparrow\downarrow$ in-cylinder pressure $\downarrow$  | CO $\uparrow$<br>NO <sub>x</sub> $\uparrow\downarrow$<br>HC $\uparrow$   |
| Singh <i>et al.</i> [21] (2021)       | LDPE (low density polyethylene) WPPO20 / D80  | Single cylinder, 4 S, diesel engine Kirlosker, model: TV1 5.2                  | Cylinder pressure $\uparrow$<br>Brake thermal efficiency $\uparrow$  | NO <sub>x</sub> $\downarrow$<br>smoke $\downarrow$   |
| Das <i>et al.</i> [20] (2020)         | Shredded medical plastic wastes 10/20/30% with diesel fuel  | Kirloskar, TV1 4 stroke single cylinder water cooled, CI engine                | Higher WPPO fraction led to: brake thermal efficiency $\downarrow\uparrow$ break specific fuel consumption $\downarrow$ break power $\downarrow$   | CO $\uparrow$<br>NO <sub>x</sub> $\uparrow$<br>UHC $\uparrow$<br>CO <sub>2</sub> $\uparrow$                    |
| Singh <i>et al.</i> [19] (2020)       | 58.6% PE (HDPE and LDPE), 26.9% PP, 8.8% PS, 5.6% PET; 10-50% WPPO in diesel blends   | Single cylinder, 4 S, Diesel engine Kirlosker, model: TV1 5.2                  | Higher WPPO fraction led to: brake thermal efficiency $\downarrow$ EGT $\uparrow$ specific fuel consumption – volumetric efficiency $\downarrow$ in-cylinder pressure $\uparrow\downarrow$ heat release rate $\uparrow\downarrow$            | CO $\uparrow$<br>NO <sub>x</sub> $\uparrow$<br>UHC $\uparrow$<br>CO <sub>2</sub> $\uparrow$                    |
| Mani <i>et al.</i> [18] (2011)        | Assorted WPPO 10/30/50/70% with diesel fuel   | Kirloskar TAF1 Four stroke, CI, air cooled, single cylinder, DI engine         | Higher WPPO fraction led to: brake thermal efficiency $\downarrow\uparrow$ EGT $\uparrow$ in-cylinder pressure $\uparrow$ ignition delay $\uparrow$ heat release rate $\uparrow\downarrow$ cylinder pressure $\uparrow$                      | CO $\downarrow$<br>NO <sub>x</sub> $\uparrow$<br>HC $\uparrow$<br>smoke $\uparrow$                             |
| Kumar <i>et al.</i> [12] (2013)       | HDPE 10/20/30/40% with diesel fuel  | CometVCT-10 four-stroke, CI, water cooled twin cylinder, constant speed engine | Higher WPPO fraction led to: brake thermal efficiency $\downarrow$ EGT $\uparrow$ break specific energy consumption $\uparrow$ mechanical efficiency $\uparrow$  | CO $\uparrow$<br>NO <sub>x</sub> $\uparrow$<br>UHC $\uparrow$<br>CO <sub>2</sub> $\downarrow$                  |
| Kalargaris <i>et al.</i> [17] (2017)  | Feedstock: styrene butadiene 47% polyester 26% clay 26% ethylene-vinyl acetate 12% rosin 6% polyethylene 1% polypropylene 1% PPO 25/50/75/90% with Diesel fuel. | AKSA A4CRX46TI four-stroke, CI, DI engine                                      | Higher WPPO fraction led to: cylinder peak pressure $\uparrow\downarrow$ cylinder pressure $\downarrow$ heat release rate $\uparrow\downarrow$ break specific fuel consumption $\uparrow$ brake thermal efficiency $\uparrow$ EGT $\uparrow$ | CO $\uparrow$<br>NO <sub>x</sub> $\uparrow$<br>UHC $\uparrow$<br>CO <sub>2</sub> $\uparrow$                    |
| Devaraj <i>et al.</i> [23] (2015)     | WPO 100%  | Kirlosker AV1 four-stroke, CI, DI engine                                       | Brake Thermal Efficiency $\downarrow$<br>Break Specific fuel Consumption $\uparrow$  | CO $\uparrow\downarrow$<br>NO <sub>x</sub> $\uparrow\downarrow$<br>HC $\uparrow$<br>smoke $\uparrow\downarrow$ |

electric efficiency than that recorded for commercial diesel due to the higher HHV of FPBO blends.

The paper [28] studied the combustion and performance characteristics of a small gas turbine fed with commercial Jet A and a 48%/52% mixture of aviation kerosene with synthetic paraffinic kerosene derived from hydro-processed esters and fatty acids (SPK-HEFA). Emission indexes for CO, CO<sub>2</sub>, and NO<sub>x</sub> in exhaust gases for HEFA/Jet A blends decreased in comparison to those of the pure Jet A. Lower fuel consumption was accomplished for the same thrust value, with the discrepancy decreasing with the increasing rotating speed. Two synthetic components of blends were tested, derived from two different materials: HEFA from camelina oil and HEFA from used cooking oil, with the addition of hydro-processed fatty acid and esters, showing a tendency to mass flow rate and CO emissions decreases [29]. An opposite tendency was observed for NO<sub>x</sub> emissions.

Chmielewski *et al.* [30] presented results of application of a fuel-water emulsion (FWE) as an alternative fuel for a micro gas turbine. The addition of water emulsion to the fuel blend was found to decrease the Jet A consumption, specific fuel consumption and turbine outlet temperature (TOT) for the wide range of engine thrust. Up to 35% reduction of NO<sub>x</sub> emission was reported at the maximum thrust. Manigandan *et al.* [31] conducted the combustion, emission and exergy analysis of a miniature gas turbine supplied by blends of Jet A with various additives, including biofuels such as rapeseed and canola-sunflower oil blended with ethanol or pentanol. The following blends were considered: R20E (70% Jet A fuel, 20% Rapeseed and 10% ethanol), CS20E (70% Jet A fuel, 20% canola-sunflower and 10% ethanol), R20P (70% Jet A, 20% Rapeseed and 10% pentanol), and CS20P (70% Jet A, 20% canola-sunflower and 10% pentanol). The fuel blends R20E, CS20E, R20P, and CS20P showed a 35%, 15%, 18%, and 10% increase in thermal efficiency of the micro-gas turbine engine, respectively. All examined fuel blends showed lower rates of emission due to the higher level of oxygen present in the samples. The blends R20E, CS20E, R20P and CS20P were recorded with a 16%, 9%, 17% and 1% decrease in average emission of NO<sub>x</sub> due to the impact of additives. Badami *et al.* [32] tested a small gas turbine supplied by three various fuels – Jet A kerosene, synthetic gas-to-liquid (GTL) fuel as well as a blend of 30% Jatropa methyl ester (JME) with 70% Jet A. The emissions index for CO was comparable for three combustibles, while the emission of unburned hydrocarbons (UHC) showed decreased trends for all biofuels. Aviation fuel combustion is characterized by lower NO<sub>x</sub> emission index values for lower rotating speeds

and higher emissions for higher speeds. Bhele *et al.* [33] studied the performance and emission characteristics of a small gas turbine fed by blends of Jatropha methyl ester (JME) with diesel. With increasing proportions of JME in blends with commercial fuel, emissions of primary air pollutants such as CO, CO<sub>2</sub> and UHC would decrease. Gürbüz *et al.* [34] showed the effect of dual-fuel diesel-hydrogen combustion on the performance as well as environmental and economic indicators of a small unmanned aerial vehicle (UAV) turbojet engine. In general, with an increase of hydrogen energy fractions (HEFs) in the entire range of engine speed, the emissions of CO and CO<sub>2</sub> were found to decrease, whereas HC and NO<sub>x</sub> emissions increased. Performance and emissions characteristics of a 30 kW gas turbine engine burning Jet A, canola methyl ester (CME), soy methyl ester (SME), recycled rapeseed methyl ester (RRME), hog-fat biofuel, and their 50% (volume) blends in Jet A were studied by Habib *et al.* [35]. With the increasing concentration of biofuel in fuel blends, the emission indexes of NO<sub>x</sub> and CO were decreased.

While reviewing the literature, it was found that there are no research papers on the combustion of fuels containing (WPPO) in a gas turbine. In this study, the performance and emission characteristics of a GTM-140 miniature gas turbine engine fueled with blends of kerosene Jet A and WPPO derived from polypropylene are investigated. From 25% to 100% of WPPO is used in WPPO/Jet A blends. Turbine exhaust temperatures, static thrust, fuel consumption and thrust specific fuel consumption, as well as thrust specific emissions of NO<sub>x</sub> and CO are measured over a broad range of turbine load and compared within the assumed range of fuel composition. The significance of this paper is to provide a better understanding of the effects of Jet A/WPPO mixtures on engine performance characteristics and exhaust emissions, as well as to assess the potential for these fuels for gas turbine applications.

## 2 Pyrolysis of waste plastics

The pyrolytic oil used as fuel in the experimental work was obtained in a semi-technical scale installation for the pyrolysis process. Taking into account the previous experience [36,37], the pyrolytic installation was modified especially for the pyrolysis of waste plastics. The installation includes the fixed bed reactor with electric heating, a panel control with a thermocouple and a system for the collection of the liquid fraction. The cylindrical

reactor has a diameter  $D = 350$  mm, height  $H = 500$  mm and is made of 3 mm thickness stainless steel. The reactor was closed using the flange connection, screwed and sealed so that the process takes place in an oxygen-free atmosphere. Before the experiment, the stainless steel reactor was placed axially in a cylindrical ceramic heating element of diameter  $D = 380$  mm with khantal heaters deployed in the reactor walls. The heat was supplied to the reactor evenly over the entire wall surface. The vermiculite insulation was placed underneath the reactor, over the entire exterior of the heating element, the reactor cover and the pipe for discharging the volatile fraction into the condenser. A scheme of the pyrolytic installation that was used in the present study is illustrated in Fig. 1.

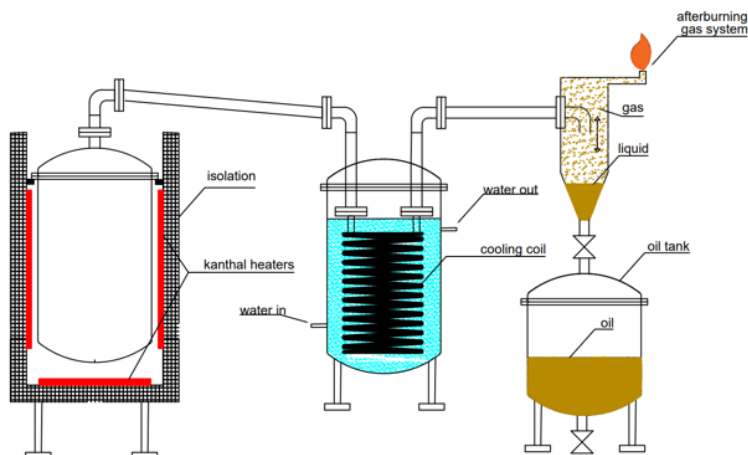


Figure 1: Scheme of the pyrolysis installation.

During the pyrolysis process, the volatile fraction was delivered from the bottom of the spiral, and after condensation, the liquid products were collected in the upper part of the spiral. The two-phase condensate mixture was directed to the tee separator and the liquid products were collected in the tank, while the gaseous fraction was burned and escaped into the atmosphere.

The plastic material was purchased from a company dealing with the recycling of plastic waste. The material was selectively separated and regranulated. In the experiment, polypropylene (PP) was subject to pyrolysis. One cycle of the pyrolysis process was conducted for 20 kg of raw material with a heating rate of  $10^{\circ}\text{C}/\text{min}$  and final temperature of  $500^{\circ}\text{C}$ . The final temperature of the process was selected on the basis of thermogravimetric



analysis, analysis of literature data and experimental work in a laboratory scale. Thermogravimetric analysis proved that below 400°C the conversion was not complete, which was also confirmed by preliminary experimental tests. The literature says that the highest liquid fraction yield can be obtained during fast pyrolysis in temperatures up to 500°C [15, 38]. The choice of the final temperature of the process is also dictated by economic considerations taking into account high energy consumption as the tests require long-term heating of the reactor. The catalyst was not used in the experiments due to extra costs involved and insignificant expected increase of the process efficiency. The reactor was thermostated at the final temperature to let the volatile fraction escape from the separator, which took approximately 6 hours. After that time, the reactor was left to cool down and the pyrolysis solid residue was removed. The liquid fraction was collected in an oil condenser with the air and water cooler. The obtained oil was clarified during a two-step process. The first stage was filtration from the suspended solid residue, like char using a peristaltic pump and a filter system containing a mesh dedicated to motor fuels. In the second stage, the oil was clarified by means of vacuum filtration using a Buchner funnel with a filter of pore size 0.13 mm. Solid particles, char and dye residue were removed from the pyrolytic oil during the filtration. The liquid fraction yield was 92% wt. for polypropylene.

### 3 Waste plastic pyrolysis oil properties

The crude PPO were investigated using gas chromatography-mass spectrometry (GC-MS) so as to identify organic compounds of the fuels. The hydrocarbons were divided according to the chain length number varying between C<sub>6</sub>–C<sub>9</sub>, C<sub>10</sub>–C<sub>24</sub> and C<sub>25</sub>–C<sub>41</sub> carbon atoms (Table 2). In the chromatographic analysis of PPO the majority of the fuel – 62.87% wt. are polycyclic and aromatic hydrocarbons (PAH) with atomic numbers C<sub>10</sub>–C<sub>24</sub>. Distillation curves of three fuels – PPO and the reference fuel Jet A,

Table 2: Carbon number division for PPO via GC-MS.

| Carbon number division           | Mass Percentage (wt. %) |
|----------------------------------|-------------------------|
| C <sub>6</sub> –C <sub>9</sub>   | 27.7                    |
| C <sub>10</sub> –C <sub>24</sub> | 62.9                    |
| C <sub>25</sub> –C <sub>41</sub> | 9.4                     |

and diesel are illustrated in Fig. 2. The GC-MS analysis of the liquid fuel sample obtained by pyrolysis of polypropylene was carried out to know the compounds present in the fuel (Fig. 3) and is summarized in Table 3. While comparing three fuel samples, different shapes of distillation curves can be observed. The Jet A fuel distillates evenly with an increasing temperature, which is related to the diversified composition of the sample containing various chain-length hydrocarbons. A quite different broken line can be observed in the distillation curve for the PPO sample, with PAH and long-chain hydrocarbons responsible for a step rise of the distillation curve at higher temperatures above 220°C.

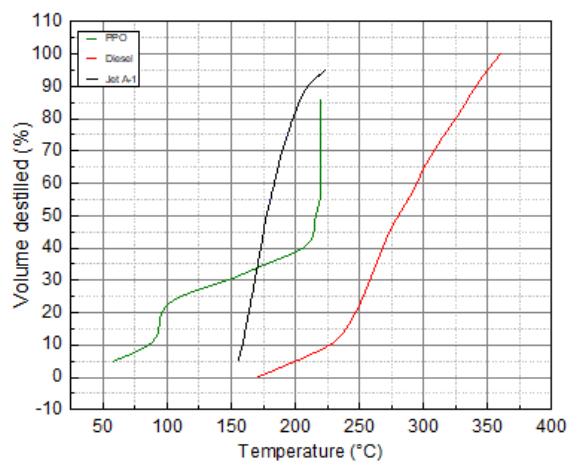


Figure 2: Distillation curves for the considered fuels.

Figure 3 presents the composition of pyrolytic oil derived from polypropylene, encompassing a variety of organic compounds such as alkanes, alco-

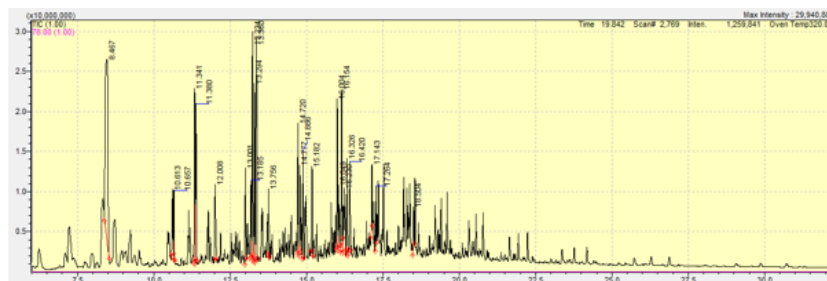


Figure 3: GC-MS spectrum of oil sample obtained at 300°C by pyrolysis of waste polypropylene.

Table 3: Compounds of PPO identified via GC-MS analysis at 300°C.

| Compounds                                | Chemical formula  | Mass percentage (%) | Molecular weight (g/mol) |
|--|---|---------------------|--------------------------|
| 2,4-Dimethyl-1-heptene                   | C <sub>9</sub> H <sub>18</sub>                                | 20.5                | 126.24                   |
| Dodecane, 4,6-dimethyl-                  | C <sub>14</sub> H <sub>30</sub>                               | 1.29                | 198.39                   |
| Heptane, 2,5,5-trimethyl-                | C <sub>10</sub> H <sub>22</sub>                               | 1.39                | 142.29                   |
| 1-Heptanol, 2,4-diethyl-                 | C <sub>11</sub> H <sub>24</sub> O                             | 3.6                 | 172.31                   |
| 2-Isopropyl-5-methyl-1-heptanol          | C <sub>11</sub> H <sub>24</sub> O                             | 3.1                 | 172.31                   |
| (2,4,6- Trimethylcyclohexyl) methanol    | C <sub>10</sub> H <sub>20</sub> O                             | 1.8                 | 156.27                   |
| Oxalic acid, cyclohexyl tetradecyl ester | C <sub>22</sub> H <sub>42</sub> O <sub>4</sub>                | 1.7                 | 370.57                   |
| Cyclohexane, tetradecyl-                 | C <sub>20</sub> H <sub>40</sub>                               | 1.3                 | 280.53                   |
| 1-Heptanol, 2,4-diethyl-                 | C <sub>11</sub> H <sub>24</sub>                               | 4.9                 | 172.30                   |
| 2-Isopropyl-5-methyl-1- heptanol         | C <sub>11</sub> H <sub>24</sub> O                             | 3.6                 | 172.31                   |
| 1-Decanol, 2-octyl-                      | C <sub>18</sub> H <sub>38</sub> O                             | 4.9                 | 270.49                   |
| Cyclododecanemethanol                    | C <sub>13</sub> H <sub>26</sub> O                             | 1.0                 | 198.34                   |
| 1-Dodecanol, 2-hexyl-                    | C <sub>18</sub> H <sub>38</sub> O                             | 2.3                 | 270.49                   |
| 1-Dodecanol, 2-octyl-                    | C <sub>20</sub> H <sub>42</sub> O                             | 1.8                 | 298.55                   |
| 1-Hexadecanesulfonyl chloride            | C <sub>16</sub> H <sub>33</sub> ClO <sub>2</sub> S            | 1.9                 | 322.95                   |
| (2,4,6-Trimethylcyclohexyl)methanol      | C <sub>10</sub> H <sub>20</sub> O                             | 0.15                | 156.26                   |
| Dotriacontyl pentafluoropropionate       | C <sub>35</sub> H <sub>65</sub> F <sub>5</sub> O <sub>2</sub> | 2.7                 | 612.90                   |
| Nonadecyl pentafluoropropionate          | C <sub>22</sub> H <sub>39</sub> F <sub>5</sub> O <sub>2</sub> | 1.1                 | 430.50                   |
| 1-Decanol, 2-hexyl-                      | C <sub>16</sub> H <sub>34</sub> O                             | 3.1                 | 242.44                   |
| Oxalic acid, butyl 1-menthyl ester       | C <sub>16</sub> H <sub>28</sub> O <sub>4</sub>                | 2.4                 | 284.39                   |
| Tetratriacontyl heptafluorobutyrate      | C <sub>38</sub> H <sub>69</sub> F <sub>7</sub> O <sub>2</sub> | 1.5                 | 690.90                   |
| Cyclooctane, 1-methyl- 3-propyl          | C <sub>11</sub> H <sub>22</sub>                               | 1.6                 | 154.29                   |
| Octatriacontyl pentafluoropropionate     | C <sub>41</sub> H <sub>77</sub> F <sub>5</sub> O <sub>2</sub> | 1.1                 | 697.00                   |
| Octatriacontyl trifluoroacetate          | C <sub>40</sub> H <sub>77</sub> F <sub>3</sub> O <sub>2</sub> | 0.9                 | 647.00                   |
| Hexatriacontyl trifluoroacetate          | C <sub>38</sub> H <sub>73</sub> F <sub>3</sub> O <sub>2</sub> | 0.8                 | 619.00                   |

hols, esters, and fluoroorganic compounds. Alkanes, such as 2,4-dimethyl-1-heptene, 4,6-dimethyldodecane, and 2,5,5-trimethylheptane are main constituents of many fossil fuels, offering high calorific value and chemical stability. Alcohols, including 1-heptanol, 2,4-diethyl-, 1-heptanol, 2-isopropyl-5-methyl-, and (2,4,6-trimethylcyclohexyl)methanol can enhance the octane rating and anti-knock properties of the fuel, but may also increase its hygroscopicity. Esters, such as oxalic acid, cyclohexyl tetradecyl ester,

dotriacontyl pentafluoropropionate, and nonadecyl pentafluoropropionate, can improve the fuel's octane rating and lubricity, but may also increase its hygroscopicity. Fluoroorganic compounds, such as tetratriacontyl heptafluorobutyrate, octatriacontyl pentafluoropropionate, octatriacontyl trifluoroacetate, and hexatriacontyl trifluoroacetate can enhance the fuel's resistance to oxidation and improve its thermal stability. This composition suggests that the pyrolytic oil has potential for fuel application, due to the presence of many compounds typical for fossil fuels. However, the physicochemical properties of such a fuel, such as calorific value, octane rating, hygroscopicity, lubricity, and thermal stability, will depend on the specific proportions of these compounds.

The basic physico-chemical properties of the considered oil were investigated using the standards and methods as defined in Table 4. Specific fuel properties as compared with those of Jet A and diesel are collected in Table 5.

Table 4: ASTM standards and methods of determination of fuel properties.

| ASTM standard | Unit              | Property            | Method  |
|---------------|-------------------|---------------------|---|
| D1298         | kg/m <sup>3</sup> | density             | density meters with U-tube oscillators (U-tube) |
| D445          | m <sup>2</sup> /s | kinematic viscosity | rheometer                                       |
| D4809-95      | MJ/kg             | calorific value     | calorimeter                                     |
| D92           | °C                | flash point         | Persky-Martens flash point test                 |

The obtained PPO is characterized by a lower density in comparison to the reference oils – Jet A1 and commercial diesel. The difference is equal to 6.5% with respect to kerosene. The higher heating value (HHV) increases with the increasing hydrogen-to-carbon ratio in oil samples as the heat of combustion of pure substances amounts to 120 MJ/kg for elemental hydrogen and 40 MJ/kg for elemental carbon. HHV of PPO equal to 44.7 MJ/kg is by approximately 3% higher than that of Jet A. The above properties have the effect of higher heat release rate and NO<sub>x</sub> emissions [17]. The WPPO flash points are below that of aviation fuel and neat diesel, and are 34°C for PPO.

Three uniform and stable blends of each considered pyrolytic oil with kerosene (Jet A) were prepared with 25%, 50%, and 75% wt. of PPO in the blends. The samples were named describing the volume of waste plastic pyrolysis oil in the Jet A blend, eg. PP25, PP50, PP75, and also PP100 as

Table 5: Physical characterization of PP oil comparison with aviation fuel and pure diesel fuel.

| Property                     | Jet A             | PPO                  | Diesel [17]    |
|------------------------------|-------------------|----------------------|----------------|
| Molecular weight (kg/kmol)   | 142               | 236.8                | –              |
| Chemical formula             | $C_{10}H_{22}$    | $C_{10,17}H_{39,55}$ |                |
| Density (kg/m <sup>3</sup> ) | 821 (at 15°C)     | 767.7                | 840            |
| Viscosity (cP)               | 1.5–2.6 (at 20°C) | 1.702                | 2.62 (at 40°C) |
| HHV (MJ/kg)                  | 43.28             | 44.7                 | 42.9           |
| Flash point (°C)             | 42                | 34                   | 59.5           |
| Sulfur (wt. %)               | 0.3               | –                    | 0.00135        |
| C (wt. %)                    | 86.15             | 89.3                 | 86.57          |
| H <sub>2</sub> (wt.%)        | 13.85             | 7.4                  | 13.38          |
| O <sub>2</sub> (wt.%)        | 0.10              | 5.5                  | 0.05           |
| Aromatic content (wt.%)      | 26                | 0                    | 29.6           |

pure PPO. The blends were chemically stable when stored in a refrigerator and also at a room temperature. The oil samples were homogeneous and transparent, their colour did not undergo visible changes even after several weeks of room-temperature exposure.

## 4 Experimental facility of the miniature gas turbine and research methodology

Given the high costs associated with experimental studies of gas turbines, several research groups have opted to explore miniature gas turbine engines [39, 40]. Research on small aircraft engines compared to stationary gas turbines is characterized by limitations such as differences in scale, operating regimes, and construction, which can affect the direct applicability of results to larger systems. However, they also offer significant advantages, including greater flexibility in testing various configurations and fuels, easier accessibility for scientific and educational research, and faster adaptation to new technologies. These aspects make research on small aircraft engines a valuable tool in the development of engine technologies, despite their limited direct comparability to large, stationary gas turbines [41, 42].

The research presented in this paper was conducted using a JETPOL GTM-140 gas turbine engine at the Institute of Fluid-Flow Machinery –

Turbine Department, Polish Academy of Sciences in Gdansk. Figure 4 illustrates a schematic diagram of the gas turbine, complete with designated measurement points.

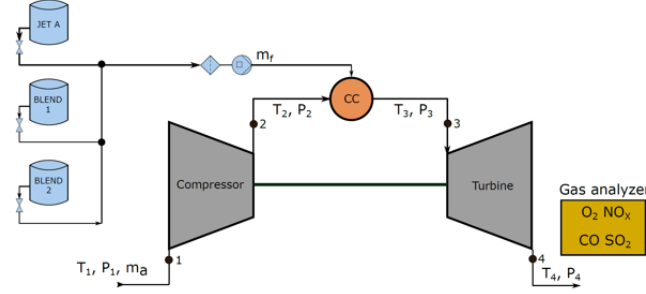


Figure 4: Gas turbine schematic diagram with measurement points [43]; T – temperature, P – pressure, 1 – before compressor, 2 – before combustion chamber, 3 – before turbine, 4 – after turbine;  $m_a$  – air mass flow,  $m_f$  – fuel mass flow.

The technical performance data for the GTM-140 miniature gas turbine engine under consideration can be found in [26]. The GTM-140 is composed of a single-stage centrifugal compressor, a single-stage axial turbine, and a reverse flow annular combustion chamber with six fuel injectors, all located on the same shaft. The experimental setup was outfitted with measurement instruments designed to capture flow and performance parameters of the gas turbine, as well as emission levels. Table 6 compiles the details of these measurements, providing the range of variation for the main parameters and emission indices, inclusive of the measurement process.

The errors associated with recalculations of certain gas turbine parameters and emission indexes from the measured values were estimated with the help of a method suggested by Moffat [44]. Errors were estimated on the basis of minimum input values and accuracy of the measuring instruments. For  $S$  – a function of independent variables  $(x_1, x_2, x_3, \dots, x_n)$ , the error of determination of the  $S$  function values can be found from equation

$$\frac{\partial S}{S} = \left[ \left( \frac{\partial x_1}{x_1} \right)^2 + \left( \frac{\partial x_2}{x_2} \right)^2 + \dots + \left( \frac{\partial x_n}{x_n} \right)^2 \right]^{0.5}. \quad (1)$$

For example, in the case of thrust specific fuel consumption (TSFC), being a ratio of the mass flow rate of fuel and thrust:

$$\text{TSFC} = \frac{\dot{m}_f}{\tau}, \quad (2)$$

Table 6: Gas turbine performance and emission measurements.

| Measured parameter   | Range                    | Unit | Device/Sensor type                         | Resolution | Uncertainty |
|--|--------------------------|------|--|------------|-------------|
| Temperatures of inlet/exit compressor/turbine sector (T1–T4) | 0–1100                   | °C   | Thermocouple K-Type                        | 1°C        | ±1°C        |
| Pressure of inlet/exit compressor and turbine sector (P1–P4) | P1 0–0.98<br>P2–P4 0–9.8 | bar  | Digital pressure transducers               | 0.01 bar   | ±1.0%       |
| Static Thrust  | 0–200                    | N    | Strain gauges                              | 1 N        | 1 mV/V      |
| Fuel volumetric flow   | 0.5–100                  | LPH  | Oval-gear flowmeter                        | 0.01 LPH   | ±0.5%       |
| Rotational speed   | 0–200 000                | rpm  | Rotational speed sensor – magnetic pick-up | 1 rpm      | ±0.5%       |

| Gas emissions   | Range   | Unit | Device/Sensor type | Resolution | Uncertainty               |
|-----------------|---------|------|--------------------|------------|---------------------------|
| Oxygen          | 0–20.95 | %    | Electrochemical    | 0.01%      | ±0.2% abs.<br>or 5% rel.  |
| Carbon monoxide | 0–5000  | ppm  | Electrochemical    | 1 ppm      | ±5 ppm abs.<br>or 5% rel. |
| Nitric oxide    | 0–500   | ppm  | Electrochemical    | 0.1 ppm    | ±5 ppm abs.<br>or 5% rel. |
| Sulphur dioxide | 0–2000  | ppm  | Electrochemical    | 0.1 ppm    | ±5 ppm abs.<br>or 5% rel. |

the maximum uncertainty can be found from the formula taking into account percentage uncertainties of measurement devices as presented in Table 6:

$$\frac{\partial \text{TSFC}}{\text{TSFC}} = \left[ \left( \frac{\partial \dot{m}_f}{\dot{m}_f} \right)^2 + \left( \frac{\partial \tau}{\tau} \right)^2 \right]^{0.5}. \quad (3)$$

From Eq. (2), the maximum error in the calculation of TSFC is equal to 0.35%. The errors connected with measured emission indexes for  $\text{NO}_x$  and CO were found to be 1.08% and 0.28%, thrust specific emission indexes for  $\text{NO}_x$  and CO – 1.43% and 0.64%, respectively.

Experimental data were recorded in stationary conditions, within the range of 50 000 rpm to 100 000 rpm for pure aviation kerosene. Process values for each rotational speed were registered upon the balancing of temperature and flow in the engine. Initially, the engine was supplied with base fuel, i.e. Jet A, then switched to alternative fuel without changing the throttle settings. The experimental results are presented as line diagrams in

a wide range of microturbine rotational speed, and also as stacked column charts for selected rotational speeds. Within the applied rpm range, the following operational data and indexes were analyzed: static thrust, fuel consumption, TSFC and emission index values for CO, CO<sub>2</sub>, and NO<sub>x</sub>.

## 5 Gas turbine performance characteristics

Figure 5 presents the static thrust and fuel mass flow rate in the gas turbine for all evaluated fuel compositions. These tests were conducted under the same throttle settings as those used for Jet A-1. Given the lower density and higher calorific value of pyrolysis plastic oil (PPO), the mass flow rate of PPO blends exhibits a decrease when compared to aviation kerosene.

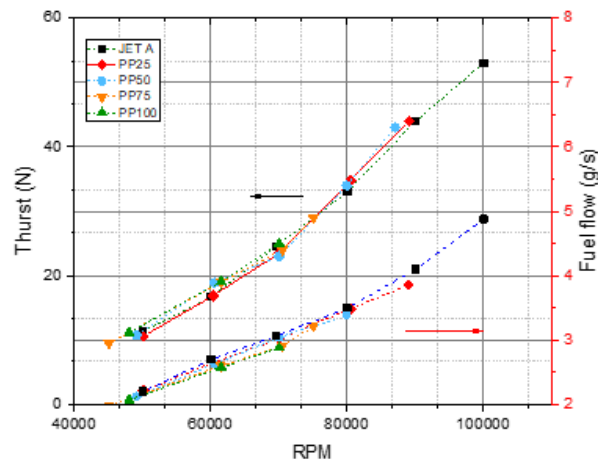


Figure 5: Static thrust and mass flow rate of fuel *vs.* turbine rotational speed for the investigated PPO/JET A blends.

The static thrust for PPO/Jet A-1 blends exhibits a slight increase with the volume share of PPO in the mixture across most of the turbine load. However, conducting tests across the full speed range proved challenging for PPO/Jet A-1 mixtures with a volume concentration of pyrolytic oil exceeding 75%. As the concentration of PPO increased, engine instability and shutdowns became more frequent. This instability accounts for the absence of characteristic data for PP75 and PP100 at rotational speeds exceeding approximately 80 000 rpm. Similar trends were noted in [28]. The thrust obtained in the test is similar, and the amount of fuel depends mainly on the calorific value of the fuel used.



Figure 6 illustrates the variation in thrust specific fuel consumption as a function of the GTM-140 engine speed. The TSFC characteristic curves for PPO/Jet A-1 blends fall below those determined for Jet A-1 across most of the turbine performance characteristics. The most significant difference between pure PPO and aviation kerosene (a TSFC reduction for pure PPO) is observed at approximately 60 000 rpm, reaching 19%. The average TSFC value for PP100 is 13.8% lower than the base fuel, a direct consequence of the higher heating value of PPO fuel. A higher LHV of WPPO results in a high heat release rate and improved combustion conditions, which has a positive effect on TSFC of the engine. Similar findings were reported in [26].

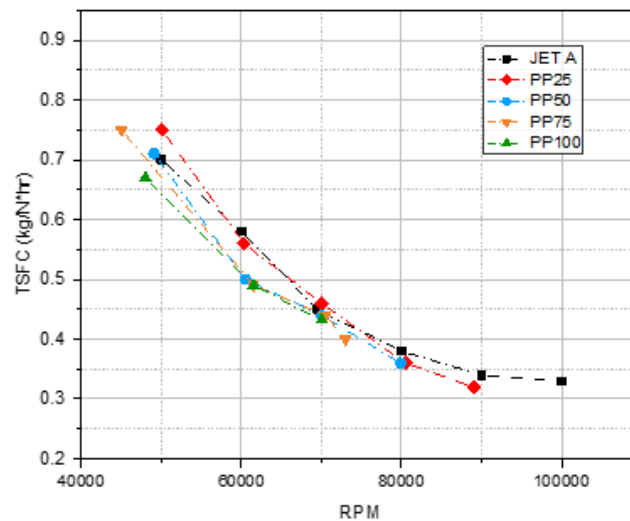


Figure 6: Thrust specific fuel consumption *vs.* turbine rotational speed for the investigated PPO/Jet A blends.

Figure 7 presents a graph depicting the exhaust gas temperature (EGT) as a function of speed. Across the entire speed range considered, EGT fluctuates between 525°C and 630°C. For all tested mixtures, this temperature decreases almost linearly with engine load, typically by 10–15°C for every approximately 10 000 rpm. This identified trend is characteristic of this type of gas turbines [28,29]. The engine outlet temperatures for the PPO/Jet A-1 blends are only marginally higher. From an operational perspective, these differences are negligible, but they could potentially influence  $\text{NO}_x$  emissions.

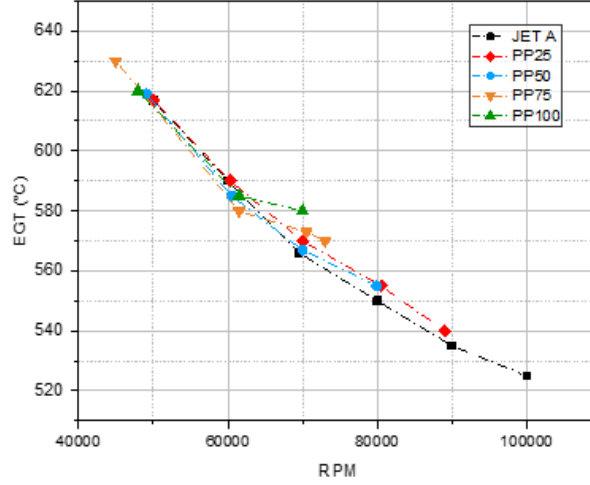


Figure 7: EGT *vs.* turbine rotational speed for the investigated PPO/Jet A blends.

## 6 Emission indexes

Upon obtaining emission concentrations in the gas exhaust, emission indexes were determined for every harmful compound of exhaust gas. The emission index for component ( $i$ ) is the mass of that component related to the mass of combusted fuel [45]:

$$EI_i = \frac{m_{i,emitted}}{m_{f,burned}}. \quad (4)$$

The emission index is regarded to assess the combustion process efficiency. For the process of hydrocarbon fuel combustion with air, the emission index can be determined for the concentrations of specific emission components (molar fraction) together with all the components containing an atom of carbon (C). Assuming that all carbon derived from the fuel was transformed into compounds of  $CO_2$  and  $CO$  contained in exhaust fumes (soot was disregarded), the emission index can be defined as [45]

$$EI_i = \left( \frac{\chi_i}{\chi_{CO} + \chi_{CO_2}} \right) \left( \frac{xMW_i}{MW_f} \right). \quad (5)$$

The first part of the equation is represented by moles of component ( $i$ ) and carbon from the fuel, whereas the part in the second bracket serves the purpose of the necessary conversion of C moles and fuel moles into

mass units. The presented emission indexes are independent of possible dilution of exhaust samples because the measured concentrations of exhaust components appear as a ratio, so the measuring error is eliminated [45]. Another way of illustrating emissions is by means of thrust specific emission indexes. The thrust specific emission indexes for  $\text{NO}_x$  and CO represent the amount of respective pollutants produced per unit turbine engine thrust [35, 46].

The emission index representing the volume of pollutants per unit of static thrust generated by the engine is expressed as

$$\text{EI}_{i,\tau} = \left( \frac{\chi_i}{\chi_{\text{CO}} + \chi_{\text{CO}_2}} \right) \left( \frac{x\text{MW}_i}{\text{MW}_f} \right) \frac{\dot{m}_f}{\tau}. \quad (6)$$

The emission index for nitrogen oxides in the function of turbine rotational speed for the investigated PPO/Jet A blends, calculated based on molar concentration in Eq. (5) is illustrated in Figure 8. The primary mechanism for the formation of nitrogen oxides in this context is the Zeldovich mechanism, also known as the thermal oxidation mechanism of neutral atmospheric nitrogen in high-temperature gas regions. This process, predominantly endothermic, escalates in efficiency at temperatures exceeding  $1577^\circ\text{C}$ , leading to a significant formation of  $\text{NO}_x$ .

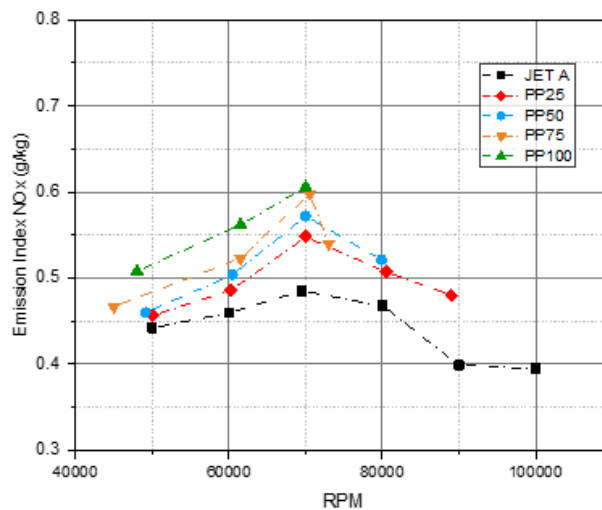


Figure 8:  $\text{NO}_x$  emission index *vs.* turbine rotational speed for the investigated PPO/Jet A blends.

In the case of PPO/Jet A fuel blends, an observed increase in  $\text{NO}_x$  emissions is notable. This increase is attributed to the elevated temperatures facilitating the Zeldovich mechanism, where nitrogen and oxygen atoms react more readily to form nitrogen oxides. On average, across the entire range of tested speeds, there is an increase in  $\text{NO}_x$  emissions ranging from 24% for the PP25 blend to 30% for the PP100 blend. This data underscores the impact of fuel composition on  $\text{NO}_x$  emission levels, influenced by the intricate interplay of temperature, fuel composition, and combustion dynamics. Other mechanisms of formation of nitrogen oxides are fuel (nitrogen in fuel), and prompt (in fuel-rich conditions), but thermal formation is the main source of  $\text{NO}_x$  emission in gas turbines.

The thrust specific  $\text{NO}_{x,\tau}$  emission index for the investigated micro gas turbine fuelled by WPPO and Jet A blends found from Eq. (5) is depicted in Figure 9. Comparable values of the TSFC for polypropylene pyrolysis oil do not strongly affect the thrust specific  $\text{NO}_{x,\tau}$  emission of investigated blends for almost the whole range of the tested turbine load. Averaging the determined curves, the specific emission index for PP100 is greater than that for Jet A only by 5.2%.

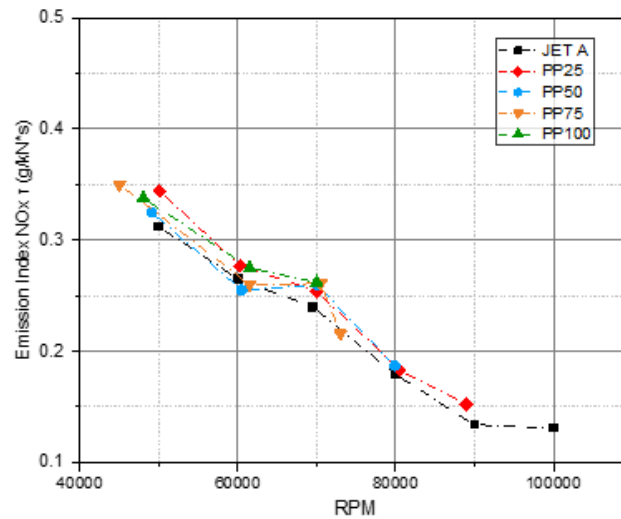


Figure 9:  $\text{NO}_{x,\tau}$  emission index *vs.* turbine rotational speed for the investigated PPO/Jet A blends.

The CO emission index of the micro gas turbine in the function of turbine rotational speed for the investigated PPO/Jett A blends is depicted

in Figure 10. For the PPO/Jet A blends, the characteristics decrease with the increasing rotational speed. The trend is not exactly clear with respect to the share of PPO in the blend. It can be assumed that the CO emission index does not considerably vary with the share of PPO. Considering definitely higher values of the molecular weight, density and viscosity for PPO with respect to Jet A, similar emission values from those fuels can be considered a satisfying result in the environmental context.

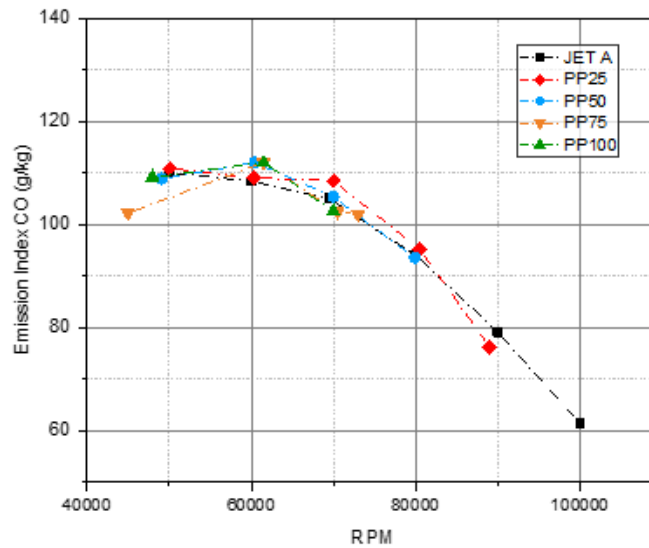


Figure 10: CO emission index *vs.* turbine rotational speed for the investigated PPO/Jet A blends.

The  $CO_{\tau}$  emission index taking into account the fuel efficiency for the investigated PPO/Jet A blends is illustrated in Fig. 11. The thrust specific  $CO_{\tau}$  emission index characteristics for PPO/Jet A blends seem to be located slightly below those for Jet A kerosene by up to 5–10%, although a few exceptions can also be noted. The research conducted suggests that the emission rates of nitrogen oxides and carbon oxides are usually higher (with an exception of  $CO_{\tau}$  emissions for PPO) when using plastic pyrolysis oils. The increase in emissions can be accepted as a method of utilization of waste plastics and turning them into energy, since a large part of plastics is not viable for recycling.

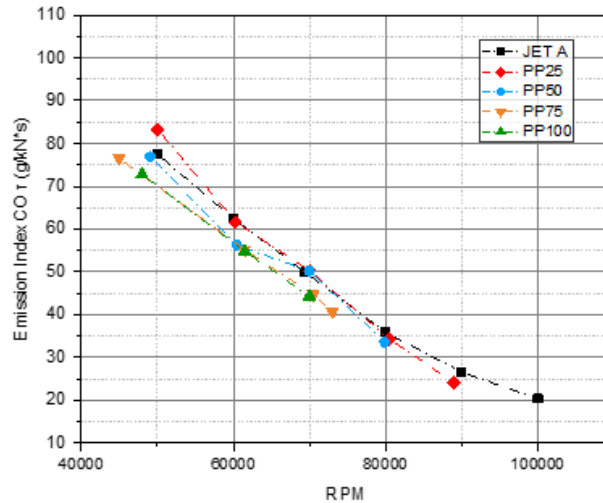


Figure 11:  $\text{CO}_\tau$  emission index *vs.* turbine rotational speed for the investigated PPO/Jet A blends.

## 7 Conclusions

This study explores the potential of managing plastic waste through its thermal conversion *via* pyrolysis, leading to the production of waste plastic pyrolysis oil (WPPO). This approach focuses on utilizing the resultant liquid fuel in powering gas turbine engines, in conjunction with aviation kerosene. WPPO represents a readily available fuel source, its abundance underpinned by the prevalence of non-recyclable waste.

Building on this, the research extends to examining pyrolytic oil derived specifically from polypropylene. Despite the general challenge of higher emissions associated with this type of pyrolytic oil, its use in micro gas turbines is considered acceptable, primarily due to its origin as a recycling by-product of polypropylene waste, which is otherwise difficult to process. This aspect of the study highlights the environmental benefits of converting challenging waste materials into valuable energy resources.

The combined approach of this research provides valuable insights into sustainable energy solutions, particularly in the management of non-recyclable plastic waste. The properties of WPPO, along with its viability as an alternative fuel, offer a promising avenue for reducing harmful emissions and pollutants. To further align with the future fuel requirements of commercial combined heat and power (CHP) systems, additional testing with

modern recuperative gas turbines can be envisioned. This holistic approach to waste management and energy utilization underscores the importance of innovative and sustainable practices in addressing environmental concerns.

The molecular weight of the derived polypropylene oil (PPO) was determined to be 236.8 g/mol, in contrast to the molecular weight of kerosene at 142 g/mol. The heating value of PPO surpasses that of Jet A by 3.3%, while its flash point is lower at 34°C. The density of the tested fuels was measured at 767.7 kg/m<sup>3</sup> for polypropylene oil.

Several fuel blends of polypropylene oil with aviation kerosene Jet A were prepared, incorporating 25%, 50%, 75%, and 100% PPO. The impact of the proportion of pyrolytic oil in PPO/Jet A fuel blends on the performance and emission characteristics of a miniature gas turbine GTM-140 was examined experimentally. The findings are presented as graphs of exhaust turbine temperature, fuel flow, static thrust, thrust specific fuel consumption (TSFC), and thrust specific emissions of NO<sub>x,τ</sub>, CO<sub>τ</sub>, measured across a broad range of micro gas turbine loads.

Drawing from the experimental results obtained from the micro gas turbine engine facility, the following conclusions can be made:

- Overall, the micro gas turbine engine when powered by polypropylene oil demonstrated superior thermal efficiency (expressed via thrust specific fuel consumption), attributable to its higher calorific value. TSFC for PPO/Jet A blends generally decreased relative to pure Jet A across most characteristics, with the greatest difference between pure PPO and aviation kerosene (a decrease in TSFC for pure PPO) observed at 60 000 rpm, reaching 19%. The average increase in thermal efficiency for pure PPO relative to Jet A was determined to be 13.8%.
- The gas turbine engine outlet temperatures for PPO/Jet A blends were marginally higher compared to pure Jet A.
- The incorporation of propylene oil (PPO) led to an increase in NO<sub>x</sub> emissions, although the largest average increase of the thrust specific NO<sub>x</sub> index observed for pure PPO relative to pure Jet A did not exceed a modest 5%.
- For PPO/Jet A blends, the thrust specific CO<sub>τ</sub> emission index was typically slightly lower by up to 5–10% in comparison to Jet A kerosene, although a few deviations from this trend were also noted.

- Polypropylene oil emerges as an attractive option, considering its superior thermal efficiency (by 13.8%), marginally lower thrust specific  $\text{CO}_\tau$  emission, and a mere 5% increase in thrust specific  $\text{NO}_{x,\tau}$  emission relative to those of Jet A.

A critical element connecting all research on turbine and combustion engines utilizing these types of fuels is the intricate and essential fuel preparation process. This process typically necessitates sophisticated techniques, such as advanced filtration, distillation, or refining systems, to ensure the fuel meets the necessary quality standards for efficient and clean combustion. The complexity and efficacy of these preparation methods play a pivotal role in determining the overall performance and environmental impact of using these fuels in gas turbines. As such, ongoing and future research should also focus on optimizing these preparation techniques to enhance the viability and sustainability of plastic-derived and other alternative fuels in energy production.

*Received 30 November 2023*

## References

- [1] Barsali S., De Marco A., Giglioli R., Ludovici G., Possenti A.: *Dynamic modelling of biomass power plant using micro gas turbine*. *Renew. Energy* **80**(2015), 806–18. doi: [10.1016/J.RENENE.2015.02.064](https://doi.org/10.1016/J.RENENE.2015.02.064)
- [2] Chiamonti D., Goumas T.: *Impacts on industrial-scale market deployment of advanced biofuels and recycled carbon fuels from the EU Renewable Energy Directive II*. *Appl. Energy* **251**(2019), 113351. doi: [10.1016/J.APENERGY.2019.113351](https://doi.org/10.1016/J.APENERGY.2019.113351)
- [3] Daraei M., Avelin A., Dotzauer E., Thorin E.: *Evaluation of biofuel production integrated with existing CHP plants and the impacts on production planning of the system – A case study*. *Appl. Energy* **252**(2019), doi: [10.1016/J.APENERGY.2019.113461](https://doi.org/10.1016/J.APENERGY.2019.113461)
- [4] Gonzalez-Salazar M.A., Venturini M., Poganietz W.R., Finkenrath M., Kirsten T., Acevedo H., *et al.*: *Development of a technology roadmap for bioenergy exploitation including biofuels, waste-to-energy and power generation & CHP*. *Appl. Energy* **180**(2016), 338–352. doi: [10.1016/J.APENERGY.2016.07.120](https://doi.org/10.1016/J.APENERGY.2016.07.120)
- [5] Januszewicz K., Kazimierski P., Suchocki T., Kardaś D., Lewandowski W., Klugmann-Radziemska E., *et al.*: *Waste rubber pyrolysis: Product yields and limonene concentration*. *Materials (Basel)* **13**(2020). doi: [10.3390/ma13194435](https://doi.org/10.3390/ma13194435)
- [6] Kazimierski P., Januszewicz K., Godlewski W., Fijuk A., Suchocki T., Chaja P., *et al.*: *The course and the effects of agricultural biomass pyrolysis in the production of high-calorific biochar*. *Materials (Basel)* **15**(2022), 3, 1038. doi: [10.3390/ma15031038](https://doi.org/10.3390/ma15031038)
- [7] GmbH PMRG (PEMRG) and CM&S.: *Final Report*, 2019.



- [8] European Association of Plastics Recycling and Recovery Organisations.: *An analysis of European plastics production, demand and waste data*. Belgium, 2015.
- [9] Anuar Sharuddin S.D., Abnisa F., Van Daud W.M.A., Aroua M.K.: *A review on pyrolysis of plastic wastes*. *Energy Convers. Manag.* **115**(2016), 308–326. doi: [10.1016/j.enconman.2016.02.037](https://doi.org/10.1016/j.enconman.2016.02.037)
- [10] Ziółkowski P., Stasiak K., Amiri M., Mikielwicz D.: *Negative carbon dioxide gas power plant integrated with gasification of sewage sludge*. *Energy* **262**(2023), 125496. doi: [10.1016/j.energy.2022.125496](https://doi.org/10.1016/j.energy.2022.125496)
- [11] Kaszuba M., Ziółkowski P., Mikielwicz D.: *Performance of cryogenic oxygen production unit with exhaust gas bleed for sewage sludge gasification and different oxygen purities*. *Arch. Thermodyn.* **44**(2023), 3, 63–81. doi: [10.24425/ather.2023.147537](https://doi.org/10.24425/ather.2023.147537)
- [12] Kumar S., Prakash R., Murugan S., Singh R.K.: *Performance and emission analysis of blends of waste plastic oil obtained by catalytic pyrolysis of waste HDPE with diesel in a CI engine*. *Energy Convers. Manag.* **74**(2013), 323–331. doi: [10.1016/J.ENCONMAN.2013.05.028](https://doi.org/10.1016/J.ENCONMAN.2013.05.028)
- [13] Kazimierski P., Hercel P., Suchocki T., Smoliński J., Pladzyk A., Kardaś D., et al.: *Pyrolysis of pruning residues from various types of orchards and pretreatment for energetic use of biochar*. *Materials (Basel)* **14**(2021), 11, 2969. doi: [10.3390/ma14112969](https://doi.org/10.3390/ma14112969)
- [14] Kantorek M., Jesionek K., Polesek-Karczewska S., Ziółkowski P., Stajnje M., Badur J.: *Thermal utilization of meat-and-bone meal using the rotary kiln pyrolyzer and the fluidized bed boiler – The performance of pilot-scale installation*. *Renew. Energy* **146**(2021), 1447–1456. doi: [10.1016/j.renene.2020.10.124](https://doi.org/10.1016/j.renene.2020.10.124)
- [15] Cai N., Xia S., Xiao H., Chen Y., Chen W., Yang H., et al.: *Distinguishing the impact of temperature on iron catalyst during the catalytic-pyrolysis of waste polypropylene*. *Proc. Combust. Inst.* **39**(2023), 1, 835–845. doi: [10.1016/j.proci.2022.06.008](https://doi.org/10.1016/j.proci.2022.06.008)
- [16] Aisien E.T., Otuya I.C., Aisien F.A.: *Thermal and catalytic pyrolysis of waste polypropylene plastic using spent FCC catalyst*. *Environ. Technol. Innov.* **22**(2021), 101455. doi: [10.1016/j.eti.2021.101455](https://doi.org/10.1016/j.eti.2021.101455)
- [17] Kalargaris I., Tian G., Gu S.: *Combustion, performance and emission analysis of a DI diesel engine using plastic pyrolysis oil*. *Fuel Process. Technol.* **157**(2017), 108–115. doi: [10.1016/J.FUPROC.2016.11.016](https://doi.org/10.1016/J.FUPROC.2016.11.016)
- [18] Mani M., Nagarajan G., Sampath S.: *Characterisation and effect of using waste plastic oil and diesel fuel blends in compression ignition engine*. *Energy* **36**(2011), 212–219. doi: [10.1016/j.energy.2010.10.049](https://doi.org/10.1016/j.energy.2010.10.049)
- [19] Singh R.K., Ruj B., Sadhukhan A.K., Gupta P., Tigga V.P.: *Waste plastic to pyrolytic oil and its utilization in CI engine: Performance analysis and combustion characteristics*. *Fuel* **262**(2020), 116539. doi: [10.1016/J.FUEL.2019.116539](https://doi.org/10.1016/J.FUEL.2019.116539)
- [20] Das A.K., Hansdah D., Mohapatra A.K., Panda A.K.: *Energy, exergy and emission analysis on a DI single cylinder diesel engine using pyrolytic waste plastic oil diesel blend*. *J. Energy Inst.* **93**(2020), 1624–1633. doi: [10.1016/j.joei.2020.01.024](https://doi.org/10.1016/j.joei.2020.01.024)
- [21] Singh T.S., Rajak U., Dasore A., Muthukumar M., Verma T.N.: *Performance and ecological parameters of a diesel engine fueled with diesel and plastic pyrolyzed oil (PPO) at variable working parameters*. *Environ. Technol. Innov.* **22**(2021). doi: [10.1016/j.eti.2021.101491](https://doi.org/10.1016/j.eti.2021.101491)

- [22] Januszewicz K., Hunicz J., Rybak A.: *An experimental assessment on a diesel engine powered by blends of waste-plastic-derived pyrolysis oil with diesel*. Energy **281**(2023). doi: [10.1016/j.energy.2023.128330](https://doi.org/10.1016/j.energy.2023.128330)
- [23] Devaraj J., Robinson Y., Ganapathi P.: *Experimental investigation of performance, emission and combustion characteristics of waste plastic pyrolysis oil blended with diethyl ether used as fuel for diesel engine*. Energy **85**(2015), 304–309. doi: [10.1016/j.energy.2015.03.075](https://doi.org/10.1016/j.energy.2015.03.075)
- [24] Chiamonti D., Oasmaa A., Solantausta Y.: *Power generation using fast pyrolysis liquids from biomass*. Renew. Sustain. Energy Rev. **11**(2007), 1056–1086. doi: [10.1016/J.RSER.2005.07.008](https://doi.org/10.1016/J.RSER.2005.07.008)
- [25] Pilavachi P.A.: *Mini- and micro-gas turbines for combined heat and power*. Appl. Therm. Eng. **22**(2002), 2003–2014. doi: [10.1016/S1359-4311\(02\)00132-1](https://doi.org/10.1016/S1359-4311(02)00132-1)
- [26] Suchocki T., Witanowski Ł., Lampart P., Kazimierski P., Januszewicz K., Gawron B.: *Experimental investigation of performance and emission characteristics of a miniature gas turbine supplied by blends of kerosene and waste tyre pyrolysis oil*. Energy **215**(2021), 119125. doi: [10.1016/j.energy.2020.119125](https://doi.org/10.1016/j.energy.2020.119125)
- [27] Buffi M., Cappelletti A., Rizzo A.M., Martelli F., Chiamonti D.: *Combustion of fast pyrolysis bio-oil and blends in a micro gas turbine*. Biomass Bioenerg. **115**(2018), 74–85. doi: [10.1016/J.BIOMBIOE.2018.04.020](https://doi.org/10.1016/J.BIOMBIOE.2018.04.020)
- [28] Gawron B., Białecki T.: *Impact of a Jet A-1/HEFA blend on the performance and emission characteristics of a miniature turboJet engine*. Int. J. Environ. Sci. Technol. **15**(2018), 1501–1508. doi: [10.1007/s13762-017-1528-3](https://doi.org/10.1007/s13762-017-1528-3)
- [29] Gawron B., Białecki T., Janicka A., Suchocki T.: *Combustion and emissions characteristics of the turbine engine fueled with HeFA blends from different feedstocks*. Energies **13**(2020), 1–12. doi: [10.3390/en13051277](https://doi.org/10.3390/en13051277)
- [30] Chmielewski M., Niszczota P., Gieras M.: *Combustion efficiency of fuel-water emulsion in a small gas turbine*. Energy **211**(2020), 118961. doi: [10.1016/j.energy.2020.118961](https://doi.org/10.1016/j.energy.2020.118961)
- [31] Manigandan S., Atabani A.E., Ponnusamy V.K., Gunasekar P.: *Impact of additives in Jet-A fuel blends on combustion, emission and exergetic analysis using a micro-gas turbine engine*. Fuel **276**(2020), 118104. doi: [10.1016/j.fuel.2020.118104](https://doi.org/10.1016/j.fuel.2020.118104)
- [32] Badami M., Nuccio P., Pastrone D., Signoretto A.: *Performance of a small-scale turboJet engine fed with traditional and alternative fuels*. Energy Convers. Manag. **82**(2014), 19–28. doi: [10.1016/j.enconman.2014.03.026](https://doi.org/10.1016/j.enconman.2014.03.026)
- [33] Bhele S.K., Deshpande N.V., Thombre S.B.: *Experimental investigation of combustion characteristics of Jatropha biodiesel (JME) and its diesel blends for gas turbine combustor*. Mater. Today Proc. **5**(2018), 11, 23404–23412. doi: [10.1016/J.MATPR.2018.11.080](https://doi.org/10.1016/J.MATPR.2018.11.080)
- [34] Gürbüz H., Akçay H., Aldemir M., Akçay İ.H., Topalçı Ü.: *The effect of euro diesel-hydrogen dual fuel combustion on performance and environmental-economic indicators in a small UAV turbojet engine*. Fuel **306**(2021), 121735. doi: [10.1016/J.FUEL.2021.121735](https://doi.org/10.1016/J.FUEL.2021.121735)
- [35] Habib Z., Parthasarathy R., Gollahalli S.: *Performance and emission characteristics of biofuel in a small-scale gas turbine engine*. Appl. Energy **87**(2010), 1701–1709. doi: [10.1016/j.apenergy.2009.10.024](https://doi.org/10.1016/j.apenergy.2009.10.024)

- [36] Lewandowski W.M., Januszewicz K., Kosakowski W.: *Efficiency and proportions of waste tyre pyrolysis products depending on the reactor type — A review*. J. Anal. Appl. Pyrolysis **140**(2019), 25–53. doi: [10.1016/J.JAAP.2019.03.018](https://doi.org/10.1016/J.JAAP.2019.03.018)
- [37] Januszewicz K., Kazimierski P., Kosakowski W., Lewandowski W.M.: *Waste tyres pyrolysis for obtaining limonene*. Materials (Basel) **13**(2020), 1–30. doi: [10.3390/ma13061359](https://doi.org/10.3390/ma13061359)
- [38] Kalargaris I., Tian G., Gu S.: *Experimental characterisation of a diesel engine running on polypropylene oils produced at different pyrolysis temperatures*. Fuel **211**(2018), 797–803. doi: [10.1016/j.fuel.2017.09.101](https://doi.org/10.1016/j.fuel.2017.09.101)
- [39] Krakos (Podwin) A., Janicka A., Molska J., Zawiślak M., Lizanets D., Białecki T., et al.: *Microfluidic-assisted toxicity studies of Jet fuels on environmental microorganisms – Towards new lab-on-a-chip sensing applications*. J. Int. Meas. Confed. **204**(2022), 112037. doi: [10.1016/j.measurement.2022.112037](https://doi.org/10.1016/j.measurement.2022.112037)
- [40] Główka M., Wójcik J., Boberski P., Białecki T., Gawron B., Skolniak M., et al.: *Sustainable aviation fuel – Comprehensive study on highly selective isomerization route towards HEFA based bioadditives*. Renew. Energy **220**(2024), 119696. doi: [10.1016/j.renene.2023.119696](https://doi.org/10.1016/j.renene.2023.119696)
- [41] Białecki T., Dzięgielewski W., Kowalski M., Kulczycki A.: *Reactivity model as a tool to compare the combustion process in aviation turbine engines powered by synthetic fuels*. Energies **14**(2021), 6302. doi: [10.3390/en14196302](https://doi.org/10.3390/en14196302)
- [42] Kotowicz J., Job M., Brzęczek M., Nawrat K., Mędrych J.: *The methodology of the gas turbine efficiency calculation*. Arch. Thermodyn. **37**(2016), 4, 19–35. doi: [10.1515/aoter-2016-0025](https://doi.org/10.1515/aoter-2016-0025)
- [43] Suchocki T., Kazimierski P., Lampart P., Januszewicz K., Białecki T., Gawron B., et al.: *A comparative study of pentanol (C5 alcohol) and kerosene blends in terms of gas turbine engine performance and exhaust gas emission*. Fuel **334**(2023), 126741. doi: [10.1016/j.fuel.2022.126741](https://doi.org/10.1016/j.fuel.2022.126741)
- [44] Moffat R.J.: *Using Uncertainty Analysis in the Planning of an Experiment*. J. Fluids Eng. **107**(1985), 173–178. doi: [10.1115/1.3242452](https://doi.org/10.1115/1.3242452)
- [45] Turns S.R.: *An Introduction to Combustion – Concepts and Applications*. McGraw-Hill, New York 2012.
- [46] Mendez C., Parthasarathy R., Gollahalli S.: *Performance and emission characteristics of a small-scale gas turbine engine fueled with ethanol/Jet A blends*. In: Proc. 50th AIAA Aerosp. Sci. Meet. Incl. New Horizons Forum Aerosp. Expo., Neshville, 9-12 Jan. 2012, AIAA, 2012–0522, 7654–7666. doi: [10.2514/6.2012-522](https://doi.org/10.2514/6.2012-522)